46th AIAA/ASME/SAE/ASEE Joint Propulsion Conference & Exhibit
25 - 28 July 2010, Nashville, TN

AIAA 2010-6767

Proof-of-Principle Detonation Driven, Linear Electric Generator Facility

Eric M. Braun,* Frank K. Lu,†
University of Texas at Arlington, Arlington, Texas, 76019

Magomet S. Sagov,‡
Neo Power Technology, Gartneriveien 4, 3300 Hokksund, Norway

Donald R. Wilson,§
University of Texas at Arlington, Arlington, Texas, 76019
and
Peter Grubyi¶
Neo Power Technology, Gartneriveien 4, 3300 Hokksund, Norway

A facility is described in which a detonation-driven piston system has been integrated with a linear generator in order to produce electricity. Their integration is made possible by integrating them into a mass-spring system that causes the piston to freely oscillate. The piston may then drive a slider containing neodymium magnets through a generator coil. Two facility setups are described. In the first setup, the piston is contained in a single mass, two-spring system where the detonation wave pressure may be modeled as a variable force. Pressure, load, and linear translation data are collected to characterize the performance of the system. Atmospheric initial mixtures of oxygen with hydrogen, propane, and methane were detonated. A load wall is removed for the second setup where a linear motor was used as a passive generator in a two-mass, four-spring system proof-of-concept test. Future work and overall potential of the facility is discussed.

Nomenclature

A	Piston face area, m^2
CJ	Chapman-Jouguet property
c_p	Constant pressure heat capacity, kJ/(kg·K)
F	Force, N
h	Enthalpy, kJ/kg
I_D	Detonation wave impulse, N·s
I_S	Spring impulse, N·s
k	Spring constant, N/m
M	mass, kg
p	Pressure, Pa

*Graduate Research Associate, Aerodynamics Research Center, Department of Mechanical and Aerospace Engineering, Box 19018. Student Member AIAA.

†Professor and Director, Aerodynamics Research Center, Department of Mechanical and Aerospace Engineering, Box 19018. Associate Fellow AIAA.

‡Chief Technology Officer.

§Professor, Aerodynamics Research Center, Department of Mechanical and Aerospace Engineering, Box 19018. Associate Fellow AIAA.

¶Chief Executive Officer and Founder.

PDE	Pulsed detonation engine
t	Time, s
T	Temperature, K
u	Velocity, m/s
x	Axial length, m
ϕ	Equivalence ratio
η_o	Overall efficiency
ρ	Density

Subscripts

0	Initial
det	Post-detonation gas property

I. Introduction

COMBUSTION via detonation releases the chemical energy of a reactive mixture with higher efficiency compared to deflagration. Among other methods, the two processes can be compared by totaling exergy losses.[1] Despite increased efficiency, utilizing detonation for propulsion systems has taken decades to develop into practical systems.[2] Recently, it has been shown that the pulsed detonation engine (PDE) can also be used for power generation and may again be more efficient than deflagration under certain circumstances.[3] Several patents have been issued for concepts that involve coupling a PDE with different systems to drive a generator and produce electricity.[4–6] Since the majority of power in the world is generated by deflagrative combustion of fuels like natural gas and coal,[7] both of which may be detonated, even small increases in the thermodynamic efficiency of power generation using these fuels is desirable.

Figure 1 shows models of a gas turbine generator and a hypothetical detonation-driven resonance generator. A typical gas turbine power generator is composed of a high pressure compressor system consisting of multiple stages to improve efficiency. Air temperature increases with the compression ratio, so a heat exchanger is usually built into the compressor system to lower the temperature prior to combustion. The coolant is then discarded and may be considered wasted heat. Once the fuel/air mixture is combusted, it drives a turbine system. One stage of the turbine is typically used to drive the compressor system, which results in an overall efficiency loss. The other stages of the turbine are connected to a gear box which is then used to generate electricity. For a PDE driven turbine, the high pressure compressor could be eliminated, which would in turn reduce the fraction of the turbine system used to run the compressor and the amount of waste heat from cooling compressed air. In a detonation-driven resonance generator, the complexity of the cycle is reduced further by eliminating the turbine system and replacing it with a resonator, which consists of a mass-spring system that absorbs the kinetic energy from the detonation wave and transfers it to a linear electric generator. Determining the feasibility of integrating a detonation-driven, mass-spring system into this power generation concept is the focus of the current work.

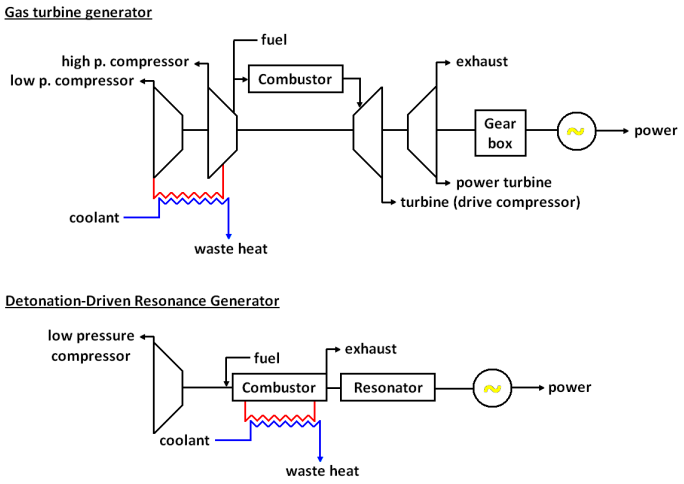

Figure 1. Model of gas turbine and detonation-driven resonance power generator systems.

An example resonator system may be designed using a two-mass, four-spring system. Many variations are possible.[8] For the system to operate effectively, the piston mass M_1 should be much greater than the magnetic slider mass M_2. Additionally, the spring constants k_1 and k_2 (associated with the piston) should be much greater than k_3 and k_4 (associated with the slider). When the detonation wave impacts the piston face, the large piston mass will be moved a short distance and oscillate for only a few cycles. However, this

minimal piston movement results in a large impulse transfer and, if the system is appropriately tuned, can cause the magnetic slider to oscillate at a resonance frequency through a fixed generator coil to continuously produce power. The magnets can be permanent and thus require no power supply. Although propulsion and power generation concepts involving detonation utilize the high temperature and pressure of the combusted mixture, this facility is novel since the force from the detonation wave is directly used to create power. While aircraft PDEs may need to operate at high frequencies to achieve steady state inlet conditions, this facility could probably be optimized around a much lower frequency. Thus, the high temperature combustion products may be more easily collected after each detonation wave and utilized further.

II. Facility Description

Two facilities have been constructed to demonstrate the feasibility of the detonation-driven linear generator. The first consists of a single mass, two-spring system and was used to understand the detonation wave interaction. The second has been configured as a two-mass, four-spring system to produce electricity and will be discussed later.

A. Preliminary Test Configuration

In the preliminary facility, a piston is mounted on one end of a linear detonation tube. An automotive spark plug (Bosch Platinum +4) ignites the mixture and creates a detonation wave which strikes the piston. The piston then acts as the free mass in a two-spring system. A schematic of this facility appears in Fig. 2. The inner diameter of the tube is 5.08 cm, and the total length is 3.05 m. The tube is constructed of stainless steel with a wall thickness of 0.64 cm. In order to let the piston oscillate freely with the springs, a support structure made of 12 radially-mounted steel rods was built around the system to secure it. Load cells (PCB model 200B05) are mounted between the end of the piston and the connector plate for the springs and between the end of the system and a rigid load plate. They are labeled LC1 and LC2 in Fig. 2. Two radial sets of six precision die springs have been implemented into the facility to support the free piston in each direction. The springs are mounted on pins to minimize buckling during the detonation wave interaction. They are also interchangeable in this facility, allowing for parametric studies with overall length and the spring constant k. In order to keep the springs from becoming detached from the assembly, a preload force of twice the anticipated detonation wave force must be applied prior to a test. Preloading is accomplished by turning nuts on the load support rods to effectively move the end of the detonation tube closer to the load plate. Consequently, the 0.75 m load support length varies slightly. A linear displacement transducer (Omega model LD621-100) labeled DT1 tracks the movement of the piston. Three pressure transducers (PCB model 111A24) are mounted at 0.152 m increments from the end of the tube. A fourth transducer is mounted on the face of the piston to capture reflected detonation wave pressure and thus accurately calculate the total impulse I from the detonation wave.

In order to enhance the parametric performance results, the piston was hollowed out so a small mass

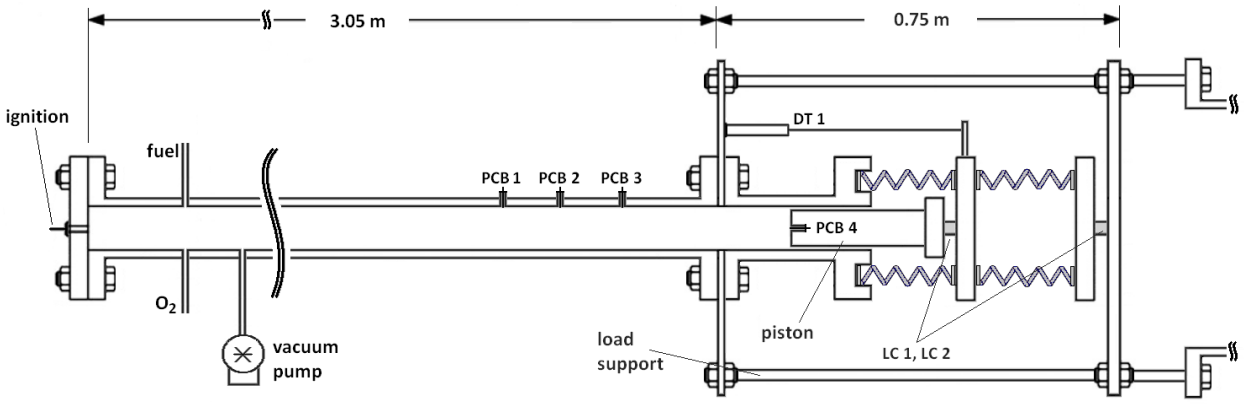

Figure 2. Schematic of the detonation tube with mass-spring components and measurement equipment indicated.

could be placed inside it. The piston itself weighs 5.035 kg while the mass weights 0.59 kg. The weight of the piston is somewhat higher than that of a normal piston since, as previously discussed, the piston mass in a complete resonance facility should be much greater than the slider mass. The piston also protrudes from the end of the tube so it may be connected to the sets of springs. The length of the piston contained in the tube varied between 8–13 cm depending upon the initial spring lengths and preload force. Teflon o-rings were used along the piston to improve sealing during the beginning of a test (when the tube was vacuumed before filling with the reactive mixture). Generally, the use of these o-rings, lithium grease, and the contact area of the piston on the tube wall was sufficient for holding a vacuum of less than 20 torr. While the tube section was constructed of stainless steel, the piston was machined from softer brass to allow for a minimal break-in time.

III. Exploratory Facility Test Results

Preliminary tests were conducted using oxygen with hydrogen, methane, and propane as fuel. The piston was used with and without the mass, and two types of 10.16 cm long springs (uncompressed) were used. Between the sets of 6 springs, k_1 and k_2 were either equal to 2.50 or 8.40 kN/cm.

A. Pressure Data

Figure 3 shows the detonation wave pressure traces from the preliminary facility where methane and hydrogen were both used as fuel under otherwise identical atmospheric initial conditions with $\phi = 1$. Detonation wave pressure and velocity measurements near Chapman-Jouguet (CJ) conditions were recorded. Thus, the post detonation wave pressure ratio of the methane/oxygen wave is approximately twice that of the hydrogen/oxygen wave. The peak pressure from the reflected detonation waves scale accordingly. The average wave speeds prior to reflection during the tests shown in Fig. 3 were about 3450 and 2600 m/s for H_2 and CH_4, respectively. The speeds indicate low to moderate overdrive ratios (1.1–1.2) of the CJ detonation process, which was observed for most of the experiments in this study.

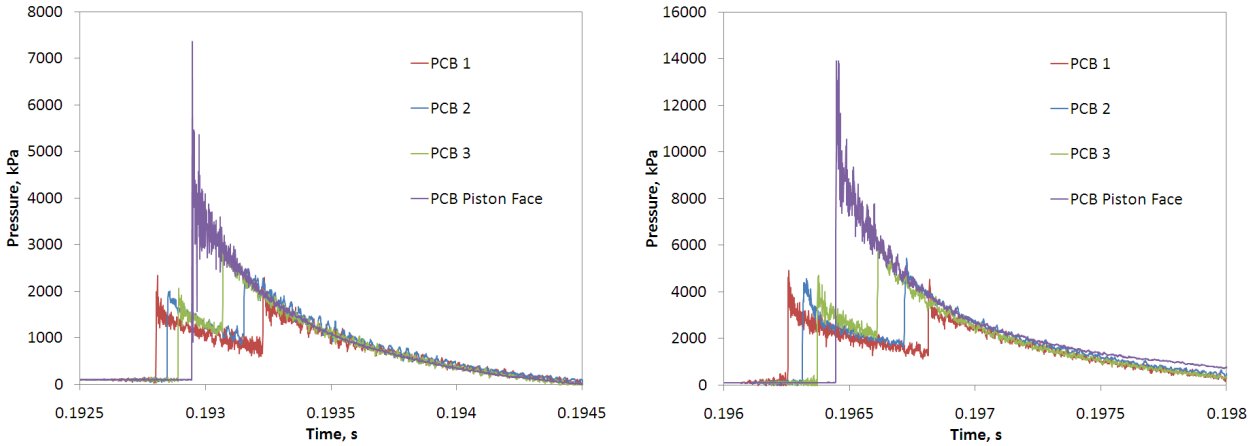

(a) $H_2 + 0.5O_2$. (b) $CH_4 + 2O_2$.

Figure 3. Detonation wave pressure traces for mixtures initially at $p_0 = 1$ atm and $\phi = 1$.

B. Piston-Spring System Data

As shown in Fig. 4, the behavior of the piston-spring system is fairly consistent while using different reactive mixtures. The force measured with load cell LC1 typically begins with a series of sharp spikes as the detonation wave strikes the piston face. The load cell LC2 measures a different force profile that does not contain a large initial spike. Instead, the force reaches a maximum value about the time the piston reaches its maximum displacement. The frequencies of the oscillations in the load cell data do not match the natural frequency of the piston-spring system, so they are probably due to waves traveling in the mechanical assembly.

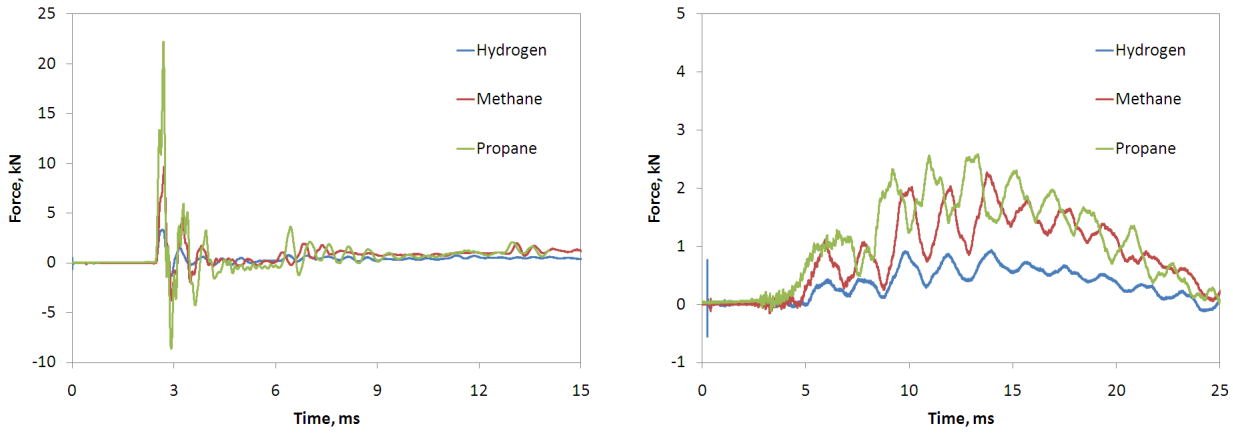

(a) Load cell LC1.

(b) Load cell LC2.

Figure 4. Piston-spring system load traces for $p_0 = 1$ atm, $\phi = 1.0$, $k = 2.50$ kN/cm, and with the piston mass.

In Fig. 5, the reactive mixture with the highest CJ pressure ratio causes the greatest displacement of the piston. The natural frequency of the system is not affected since it is based on the spring stiffness and piston mass. The piston displacement does not immediately return to the initial position because the pressure of the non-vented detonation products is above the initial value. Although this piston-spring system is underdamped and thus loses energy with each oscillation, the behavior is acceptable because the impulse may be quickly transferred to the longer and weaker springs with the slider in a generator mode. Figure 5(b) shows that the detonation wave acts on the piston face for a relatively short time compared with the oscillations in the piston-spring system, so it may be possible to model the system by replacing the detonation wave with an impulse function.

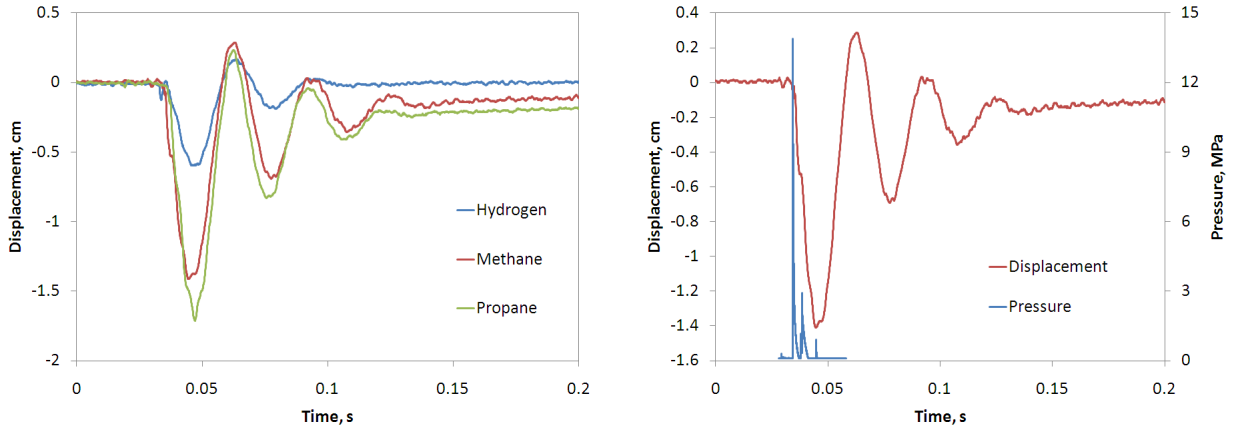

(a) Piston displacement comparison.

(b) Displacement and pressure data for a methane case.

Figure 5. Piston-spring system displacement traces for $p_0 = 1$ atm, $\phi = 1.0$, $k = 2.50$ kN/cm, and with the piston mass.

As expected, Fig. 6(a) shows an increase in the spring stiffness reduces the displacement of the piston for the example methane/oxygen case. The result of increasing the piston mass as shown in Fig. 6(a) is an increase in piston displacement. An increase in piston displacement also means more energy is stored in the springs, so adding mass to the piston can be beneficial.

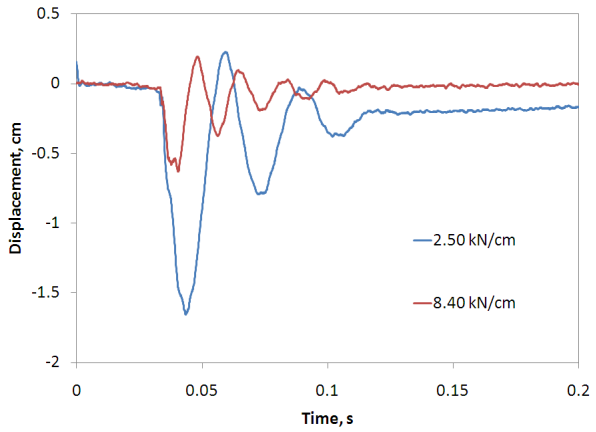

(a) Variation of spring constant k (C_3H_8-O_2 mixture).

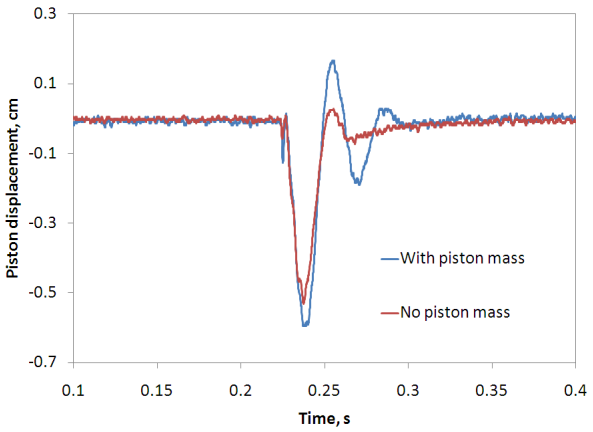

(b) Variation of the piston mass (H_2-O_2 mixture).

Figure 6. Additional mass-spring system parametric variations with $p_0 = 1$ atm and $\phi = 1.0$.

C. Variation of H_2-O_2 Equivalence Ratio

A series of tests were conducted using H_2–O_2 mixtures with $k = 2.5$ kN/cm, $p_0 = 1$ atm, and without the piston mass. The equivalence ratio was determined using partial pressures collected before and after filling the tube with the individual reactants. The error in ϕ for each test has been calculated using a 95% confidence interval. In Fig. 7(a), the equivalence ratio was successfully varied between 0.5 and 2.2 while maintaining a detonation wave. Interestingly, piston displacement actually increased as ϕ was lowered. As shown in Fig. 7(b), a linear trend is seen between maximum displacement and the mass of the detonation products as calculated by the program CEA.[9]

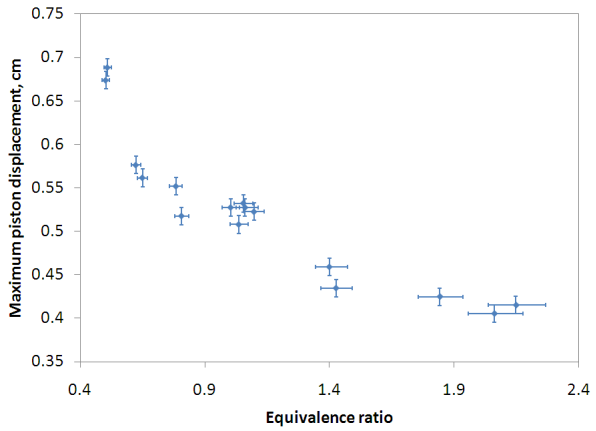

(a) Displacement versus ϕ.

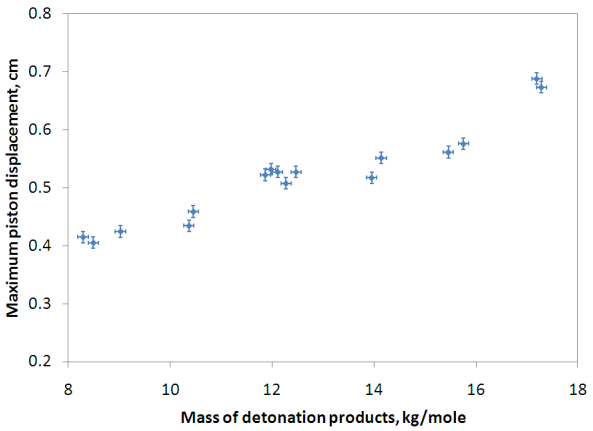

(b) Displacement versus mass.

Figure 7. Piston displacement trends for a variation of equivalence ratio for atmospheric pressure H_2–O_2 tests.

The impulse of a detonation tube has been measured and modeled in the literature.[10,11] The impulse is a function of pressure and the exhaust area of the tube. However, the addition of the piston-spring system adds additional factors and the conservation of momentum equation must be solved in the form of Eq. (1).

$$p(t)_{det}A + \rho(t)_{det}Au(t)^2_{det} = F(x)_{spring} + \frac{1}{2}Mu(t)^2_{piston} \tag{1}$$

Above, the pressure, density, and velocity values acting on the piston face must be known. On the RHS, the force from the springs (as they compress) and the piston kinetic energy are accounted for. Free pistons have previously been used to create high-enthalpy test facilities with detonation driver sections.[12] However,

it does not appear that such a momentum conservation analysis has been performed, perhaps because the facility optimization was empirical. Finding the density and velocity of the detonation products on the piston face will require a detailed analysis and will be left for future development. The trend in Fig. 7(a) probably will not be as favorable for other gas mixtures as it is with hydrogen and oxygen. According to Fig. 8, the increase in impulse for fuel-lean H_2–O_2 mixtures is benefitted by the nearly constant CJ pressure ratio to $\phi = 0.5$ and a steep rise in overall mass of the products. Note that the data is normalized with respect to the pressure ratio and mass for stoichiometric detonation.

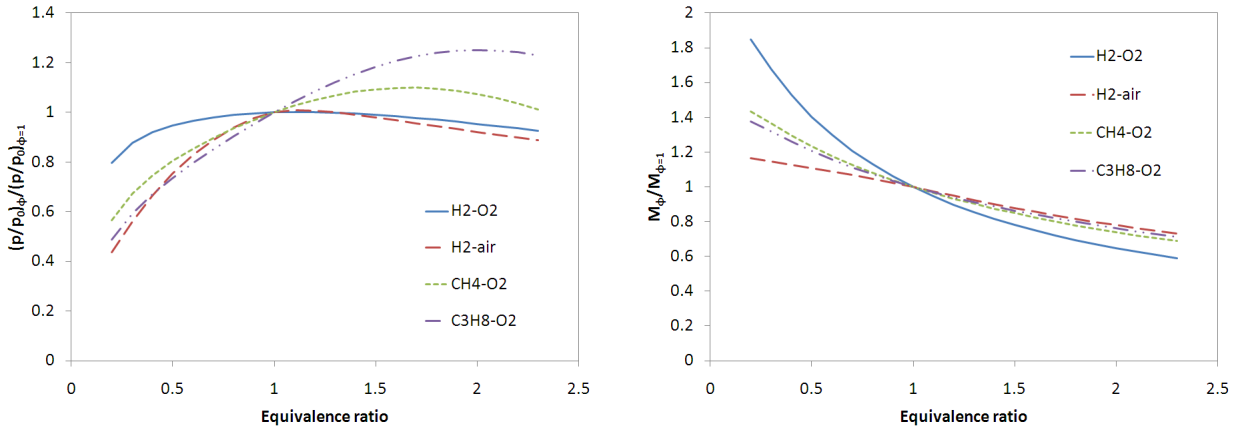

(a) Pressure ratio.

(b) Mass (kg/mole).

Figure 8. CJ properties versus equivalence ratio for several reactive mixures.

IV. Exploratory Facility Performance Analysis

A. Specific Impulse

The impulse of the detonation wave can be measured using the flush-mounted pressure transducer on the piston face and Eq. (2). The time used for the force integration begins with the rise in pressure from the detonation wave and ends after the rarefaction wave and any reflected waves occur.

$$I_D = \int F(t)dt = \int [p(t)A]_{piston}\, dt \tag{2}$$

The detonation wave impulse measurement is not always consistent. Reflected waves and heating of the transducer sometimes lead to non-physical distortions in the pressure reading and a large variation in I_D for similar initial conditions. A second, and more consistent, impulse may be calculated as the piston mass moves and acts on the set of radial springs. Using Hooke's law, $F = -kx$, the impulse may be calculated using Eq. (3). Here, dt is specified as the time in which the piston moves from its initial location to its maximum displacement point.

$$I_S = \int F(t)dt = \int [kx(t)]_{springs}\, dt \tag{3}$$

The spring specific impulse results from the H_2–O_2 tests where ϕ was varied appear in Fig. 9(a). Both fuel-based (I_S/M_f) and mixture-based ($I_S/(M_f + M_o)$) impulses are calculated. Air will be used as an oxidizer in a practical facility, so its performance should trend similar to the fuel-based results. The fuel-based specific impulse follows a trend similar to what was seen with maximum piston displacement and reaches about 4500 seconds for $\phi = 0.5$. The mixture-based impulse remains fairly steady throughout the variation in ϕ because the decline in piston displacement is offset by the decline in mass of the detonation products. Although the impulse produced with methane is higher than with hydrogen fuel, the resulting specific impulse in Fig. 9(b) is lower. Although adding the piston mass appears to increase the maximum displacement of the piston, it does not noticeably increase specific impulse.

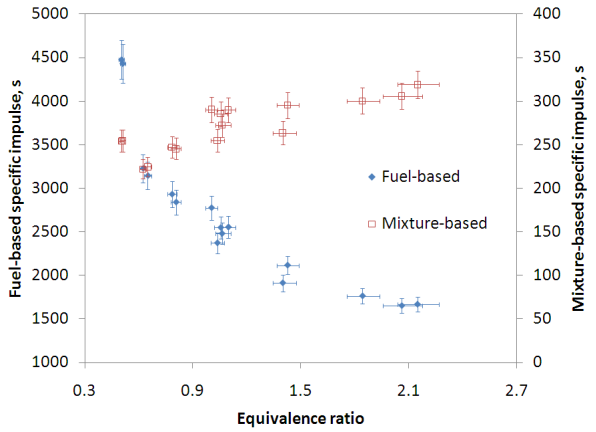

(a) Variation in H_2–O_2 equivalence ratio.

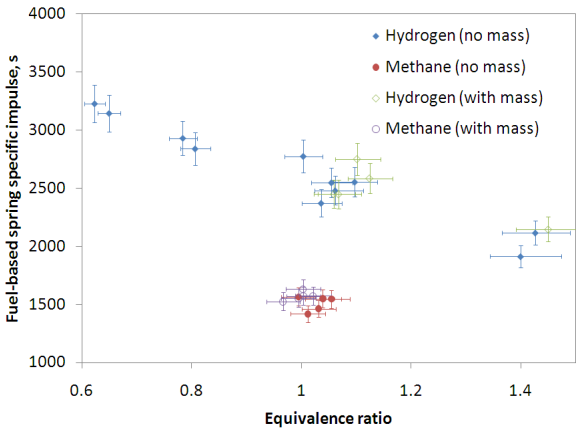

(b) Methane and Hydrogen results with and without the piston mass.

Figure 9. Specific impulse data with $p_0 = 1$ atm and $k = 2.50$ kN/cm.

B. Specific Energy and Efficiency

The energy stored in a spring is equal to $k(\Delta x)^2/2$. Thus, it is possible to calculate specific energy output of the detonation-driven system. In Fig. 10(a), the same experimental cases from Fig. 9(b) are plotted in terms of specific energy output versus equivalence ratio. Despite the fact that adding mass to the system did not result in an increase in specific impulse, the specific energy output rises significantly. For the hydrogen cases where $\phi = 1$, a 10% increase in mass results in about a 25% increase in specific energy. Although the specific impulse of methane is lower, the specific energy is nearly doubled due to the higher CJ pressure ratio and mass of the detonation products. Figure 10(b) shows the tests with propane creating slightly higher specific energy values than methane. Spring constants of 2.50 and 8.40 kN/cm were used. Contrary to expectations, the use of 8.40 kN/cm springs drastically reduced the specific energy output. Optimization of this facility clearly requires more parametric studies in conjunction with Eq. (1).

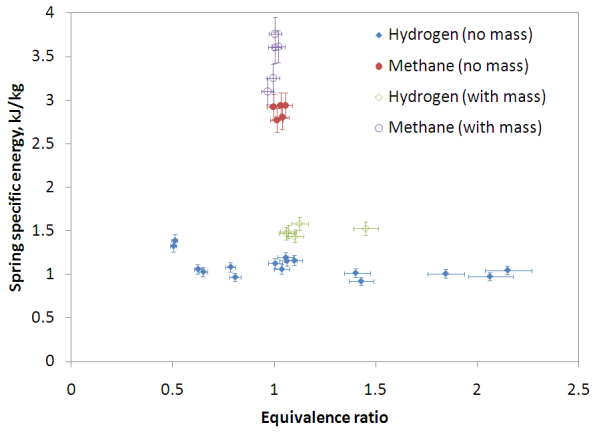

(a) Hydrogen and methane using $k = 2.50$ kN/cm with and without the piston mass.

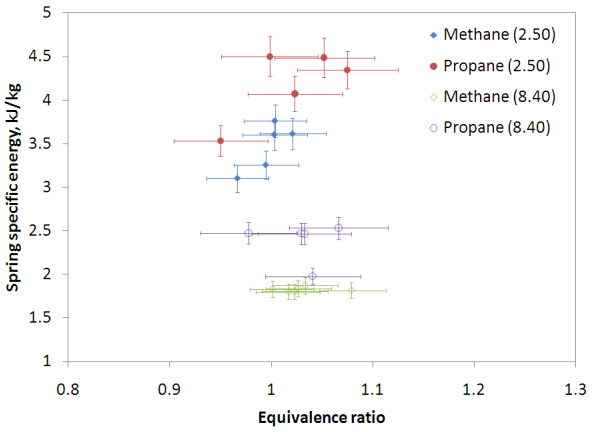

(b) Methane and propane with the piston mass for two k values.

Figure 10. Specific energy data for selected H_2, CH_4, and C_3H_8 cases.

The overall efficiency of the facility can be determined using the spring energy and the change in enthalpy of the detonation tube mixture. In order to calculate the final enthalpy of the detonation tube mixture, a model that estimates the rarefaction wave properties behind the detonation front was utilized with Cantera and a detonation toolbox.[13–15] The density distribution in the tube just prior to reflection of the wave off of the piston face was then averaged, with the other properties calculated from perfect gas relations. Overall

efficiency is expressed in Eq. (4).

$$\eta_o = \frac{\frac{1}{2}k\left(\Delta x_{max}\right)^2 + c_{p,det}T_{det}M_{det}}{\left(h_{det} + \frac{V_{det}^2}{2} - h_0\right)M_{det}} \tag{4}$$

Efficiencies using the fuels from the experimental studies are listed in Table 1 for combustion with oxygen and air. The spring energy values were averaged from the experiments using the piston mass along with the 2.50 kN/cm springs. Unfortunately, the spring energy makes a negligible contribution to overall efficiency for this facility. The enthalpy of the detonation products left in the tube results in a thermodynamic efficiency of about 60–65%. For a two-mass, four-spring resonator system where the piston does not move far, the detonation products will have to be collected and utilized in a hybrid turbine in order for this power generation concept to be thermodynamically competitive. Reviewing Eq. (4), it is apparent that the spring energy is transferred from the ${V_{det}}^2/2$ term. Although hydrogen is usually viewed as the most efficient fuel available for aircraft, the hydrocarbon fuels performed better in this study because of a higher CJ pressure ratio.

Table 1. Detonation tube and piston-spring system efficiency calculations (T_0 = 300 K, p_0 = 1 atm).

Mixture ($\phi = 1$)	$c_{p,det}T_{det}$, kJ/kg	Detonation η_o	Spring Energy, kJ/kg
$2H_2 + O_2$	9952	0.650	1.50
$2H_2$ + air	4247	0.630	–
$CH_4 + 2O_2$	6860	0.638	3.47
CH_4 + 2(air)	3473	0.624	–
$C_3H_8 + 5O_2$	6455	0.630	4.19
C_3H_8 + 5(air)	3429	0.622	–

V. Linear Generator Proof-of-Concept Test and Results

The exploratory facility was rearranged for a qualitative proof-of-concept test to demonstrate power generation with a two-mass, four-spring system. Figure 11 shows the setup. The load cell LC2 was removed and a new load plate was added that allowed for a spring to be placed through the center. A LinMot P01–23x80 linear motor was placed between the two low k springs and mounted on Lexan windows secured to the new load plate. The slider for the linear motor contains neodymium magnets, and it can generate up to a 44 N force.

The input wiring to the motor was rearranged into the two-phase generator circuit shown in Fig. 12(a). The power generated from each phase of the motor, which contains a frequency dependent on that of the slider-spring system, is rectified and filtered to a DC signal. Low voltage diodes and capacitors were used.

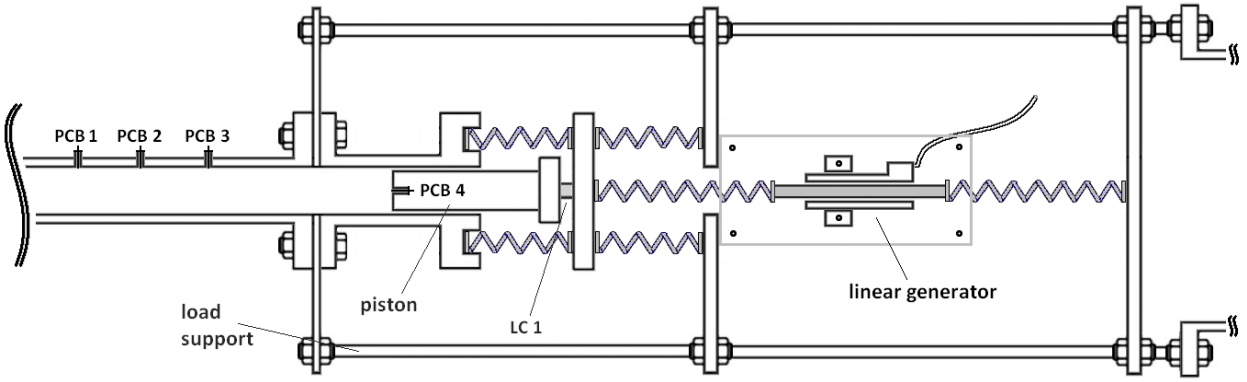

Figure 11. Schematic of the linear generator setup.

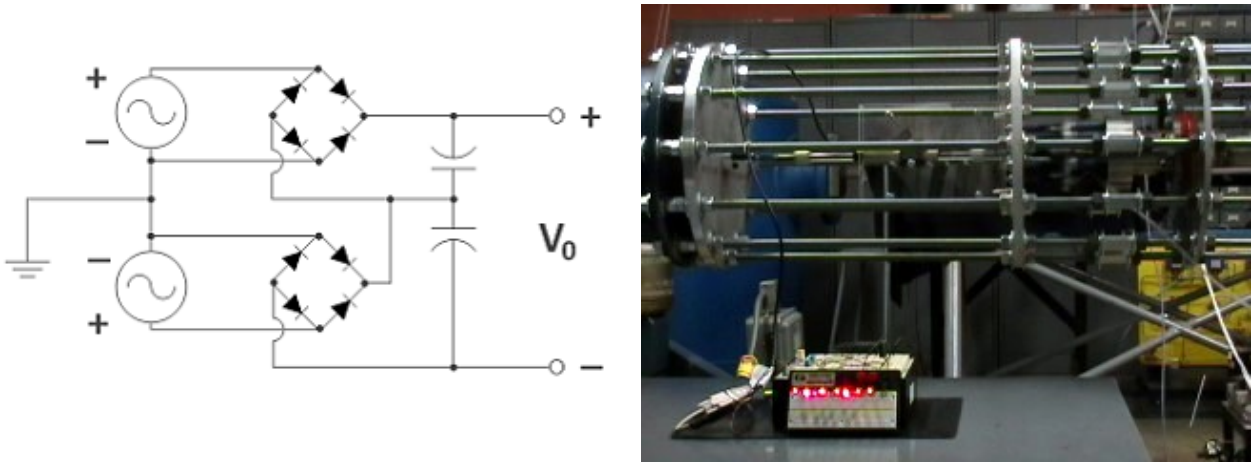

(a) Circuit diagram.

(b) LEDs actuated by the detonation driven generator.

Figure 12. Linear generator experimental setup.

The combined capacitance used for the experiment shown in Fig. 12 was about 1000 μF. In that experiment, LEDs were assembled in parallel with the circuit output voltage.

During testing, a small amount of power was generated by the detonation wave acting on this system. For a single-shot system, the impulse from the piston onto the slider should cause it to oscillate so the LEDs would be lit for a few seconds. However, the low k springs tended to buckle sideways since keeping all the components of this facility aligned is troublesome. The buckling problem was mitigated for the piston-spring system using the sets of radially distributed springs, but only one linear motor was available for this study. The piston oscillation was not significantly affected by the energy transfer to the slider, so it is probable that many generator elements will have to be connected to this system so the piston can transfer all of its available energy before it dissipates.

VI. Conclusions and Future Prospects

This preliminary experimental study of a detonation-driven, linear electric generator facility has highlighted several trends that will be characteristic of future facility designs:

- Maximum piston displacement, which affects specific impulse and energy, is equally dependent on all terms of the conservation of momentum equation. As an example, fuel-lean H_2–O_2 mixtures have increased performance because the wave pressure is nearly constant while mass increases.
- Parametric studies of performance with different piston masses and k values show a facility will require careful optimization of these parameters working together.
- An increase in the piston mass caused a rise in specific energy output but not specific impulse. This trend can be likened to high I_{sp} plasma rockets that actually have very low thrust. Specific energy increased because the increase in piston mass improved momentum transfer in the system. Specific impulse did not change because of the increased time for the springs to reach their maximum displacement.
- Although the specific energy output of the current system has proven to be low, the spring-based specific impulse values are promising. Consequently, the authors believe overall efficiency can be increased significantly with an optimized system.

The low overall efficiency contribution from the detonation wave acting on the piston was not totally unexpected for such a preliminary facility, but it does show that a constant area PDE driver may not be optimal because of the enthalpy of the leftover detonation products. Novel ideas for managing the enthalpy terms from Eq. (4) are needed. Instead of using a constant area tube, a PDE driver section could be

connected to a nozzle attached to a downstream section with atmospheric pressure working gas. Using this PDE driver could transfer more of the static enthalpy to kinetic energy. Regarding future work, several steps must be taken to further develop this detonation-driven, linear electric generator concept:

- First, the experimental results from this facility should be modeled. Doing so will allow for the piston mass and spring stiffness to be optimized according to Eqs. (1) and (4). Linear power generation could also be added to the model, where electromagnetic effects will contribute to damping in a two-mass, four-spring resonator system.
- The two-mass, four-spring resonator system was designed so the piston would connect to stiff springs to store energy before it was collected by the linear generator components. The desirable travel length for the piston was set to a few centimeters for this study, which was considered necessary to reduce mechanical wear to the system. Future design efforts will focus on two concepts. The first is a hybrid system where the hot detonation products are collected and used in a power turbine. The second concept uses a nozzle where the detonation products expand into a working gas, thereby transferring the detonation wave static enthalpy into kinetic energy.
- The next facility will be developed to include a pulsed detonation engine instead of a single-shot tube. The linear generator can be tuned to resonate with a given detonation wave frequency to generate steady power. Water-cooling, exhausting, and purging the PDE will become necessary, but are feasible with operating frequencies of 30 Hz or less. Fuel/oxygen mixtures were used for this facility, but future facilities will use fuel/air mixtures. The use of hydrocarbon-air mixtures will result in much larger facilities since the tube diameter must be larger than the detonation cell sizes.

Acknowledgments

The current work has been supported by a sponsored research agreement between Neo Power Technology and the University of Texas at Arlington. The authors would like to thank Nathan Dunn and Rodney Duke for assistance with testing and manufacturing of the facility.

References

[1]Petela, R., "Application of Exergy Analysis to the Hydrodynamic Theory of Detonation in Gases," *Fuel Processing Technology*, Vol. 67, No. 2, 2000, pp. 131–145.

[2]Kailasanath, K., "Review of Propulsion Applications of Detonation Waves," *AIAA Journal*, Vol. 38, No. 9, 2000, pp. 1698–1708.

[3]Bellini, R. and Lu, F. K., "Exergy Analysis of a Pulse Detonation Power Device," *private communication*.

[4]Bussing, T. R. A., "Pulse detonation electrical power generation apparatus with water injection," *U.S. Patent No. 6,062,018*, May 16, 2000.

[5]Schick, L. A. and Dean, A. J., "Hybrid fuel cell-pulse detonation power system," *U.S. Patent No. 7,150,143*, December 19, 2006.

[6]Lu, F. K. and Wilson, D. R., "Scalable Power Generation Using a Pulsed Detonation Engine," *U.S. Patent No. 7,340,903*, March 11, 2008.

[7]Doman, L., "International Energy Outlook 2009," Tech. Rep. DOE/EIA-0484(2009), Energy Information Administration, Washington, DC, May 2009.

[8]Sagov, M. S., "Energy Converter," *U.S. Patent No. 6,759,755*, July 6, 2004.

[9]McBride, B. J. and Gordon, S., "Computer Program for Calculation of Complex Chemical Equilibrium Compositions and Applications I. Analysis," Tech. Rep. NASA-RP1311, National Aeronautics and Space Administration, Cleveland, OH, Oct. 1994.

[10]Wintenberger, E., Austin, J., Cooper, M., Jackson, S., and Shepherd, J. E., "Analytical Model for the Impulse of Single-Cycle Pulse Detonation Tube," *Journal of Propulsion and Power*, Vol. 19, No. 1, 2003, pp. 22–38.

[11]Cooper, M., Jackson, S., Austin, J., Wintenberger, E., and Shepherd, J. E., "Direct Experimental Impulse Measurements for Deflagrations and Detonations," *Journal of Propulsion and Power*, Vol. 18, No. 5, 2002, pp. 1033–1041.

[12]Lu, F. K., Wilson, D. R., Bakos, R. J., and Erdos, J. I., "Recent Advances in Detonation Techniques for High-Enthalpy Facilities," *AIAA Journal*, Vol. 38, No. 9, 2000, pp. 1676–1684.

[13]Endo, T. and Fujiwara, T., "A simplified analysis on a pulse detonation engine model," *Transactions of the Japan Society for Aeronautical and Space Sciences*, Vol. 44, No. 146, 2002, pp. 217–222.

[14]Goodwin, D., "Cantera: Object-oriented Software for Reacting Flows," *http://code.google.com/p/cantera*, accessed June 30, 2009.

[15]Browne, S., Ziegler, J., and Shepherd, J. E., "Numerical Solution Methods for Shock and Detonation Jump Conditions," Tech. Rep. GALCIT Report FM2006.006, California Institute of Technology, Pasadena, CA, Aug. 2008.